ELSEVIER

Journal of Power Sources 62 (1996) 101–105

JOURNAL OF POWER SOURCES

# New tin-containing spinel sulfide electrodes for ambient temperature rocking chair cells

M.A. Cochez [b], J.C. Jumas [b], P. Lavela [a], J. Morales [a], J. Olivier-Fourcade [b], J.L. Tirado [a,*]

[a] *Laboratorio de Química Inorgánica, Facultad de Ciencias, Universidad de Córdoba, avda. San Alberto Magno s/n, 14004 Córdoba, Spain*

[b] *Laboratoire de Physicochimie des Materiaux Solides, Université Montpellier II, place E. Bataillon, 34095 Montpellier 5 Cedex, France*

Received 3 January 1996; revised 5 March 1996; accepted 19 March 1996

**Abstract**

Spinel compounds with $Cu_2CoSn_3S_8$ and $CuCoSn_3S_8$ stoichiometries were evaluated as the active electrode materials in lithium anode and 'rocking chair'-type cells. For lithium cells using $CuCoSn_3S_8$ cathodes, the current–composition curves obtained by step potential electrochemical spectroscopy revealed a first $Co^{III}/Co^{II}$ reduction peak during cell discharge at about 1 F $mol^{-1}$, which is not observed for the $Cu_2CoSn_3S_8$ composition. Lithium-ion diffusion coefficients were also larger in this interval. The galvanostatic cycling behaviour in the 2–2.5 V potential window leads to little capacity losses after the first cycle when using $CuCoSn_3S_8$ electrodes. Three electrode sulfide/$LiClO_4$(PC)/$LiCoO_2$ rocking chair cells using lithium auxiliary electrode were examined by galvanostatic cycling experiments. When the cells are cycled in the 1.5–2.5 V interval, cell capacity (≤5 mAh $g^{-1}$) remains basically unaffected between the second and tenth cycles. The presence of $Sn^{IV}$ ions in these solids which are suitable for reduction at lower voltages may be of interest as overdischarge protection.

*Keywords:* Capacity; Cycling; Lithium insertion electrode; Lithium-ion cells

## 1. Introduction

Since the early 1980s, the search for a suitable negative electrode in rocking chair cells has deserved the interest of different researchers [1–3]. Although a significant improvement was achieved by the use of carbon electrodes in lithium-ion cells [4–7], research in this area has allowed the use of other inorganic host lattices, such as lithium-rich spinel oxides [8] or layered chalcogenides [9], as promising low-potential electrodes. Similar to spinel oxides, spinel chalcogenides contain a non-negligible number of empty sites to host lithium ions while their three-dimensional structures allow an isotropic lattice expansion on lithium insertion. Moreover, the size of the 'bottle neck' for lithium-ion diffusion is now defined by the size of S atoms, which is large enough to allow appropriate diffusivities through a system of intercrossed empty channels [10], while inhibiting solvent cointercalation, a problem usually found in the use of two-dimensional intercalation electrodes, as recently confirmed in graphite by scanning tunneling microscopy (STM) techniques [11]. Moreover, removal of certain ions from the structure of spinel sulfides by chemical procedures such as those proposed in the pioneering work of Schöllhorn and Payer [12], allows an enhanced lithium diffusivity [13,14].

In a recent work [15], we described the synthesis and insertion properties of compounds with $Cu_2MSn_3S_8$ (M = Mn, Fe, Co, Ni) stoichiometry. These materials were shown to insert lithium electrochemically. On the other hand, copper could be extracted from their structures by chemical procedures, giving rise to enhanced insertion properties by decreasing the repulsions between copper ions in tetrahedral sites and the inserting lithium ions. Copper extraction takes place with simultaneous cobalt oxidation, thus leading to a possible control over cell voltage when using these compounds as an active electrode material.

Here, the thermodynamic and kinetic properties of the electrochemical lithium insertion process into $Cu_2CoSn_3S_8$ and $CuCoSn_3S_8$ are studied in order to select the best material to be combined with 'standard' $LiCoO_2$ cathodes in rocking chair cells. The cycling properties of the resulting cells in two- and three-electrode assemblies are also evaluated.

## 2. Experimental

### 2.1. Materials

Powdered samples of $Cu_2CoSn_3S_8$ were obtained from stoichiometric amounts of the concerning elements in evac-

* Corresponding author.


*PII* S0378-7753(96)02409-3

uated quartz tubes. Intimate mixtures of the elements were heated at 300 °C for 24 h and then the temperature was increased to 750 °C. After 8-day treatment periods, the products were quenched to room temperature, reground and kept into an argon atmosphere dry box.

The copper-extracted product $CuCoSn_3S_8$ was prepared by suspending about 1 g of $Cu_2CoSn_3S_8$ in an excess of 0.1 M $I_2/CH_3CN$ solution at 50 °C while magnetic stirring for a period of ten days. The solid product was then washed with dry acetonitrile and stored inside the dry box.

$LiCoO_2$ powders were prepared from lithium and cobalt carbonates by the conventional procedure described by Johnston et al. [16].

### 2.2. Electrochemical experiments

Two different cell assemblies were used. The electrochemical lithium insertion properties of the sulfides were evaluated versus lithium metal in two-electrode $Li/LiClO_4(PC)$/sulfide cells. Rocking-chair sulfide/$LiClO_4(PC)/LiCoO_2$ cells were also evaluated in three-electrode assemblies, using lithium metal as the reference electrode. For these purposes a MacPile multichannel system was used, which allows the simultaneous recording of auxiliary and working voltages. Pellet electrodes with sulfide-active material were prepared by pressing, at 200 MPa, a mixture of 90 wt.% sample and 10 wt.% polytetrafluoroethylene (PTFE) to improve the mechanic properties of the electrode. For $LiCoO_2$ electrodes, pellets were prepared by using a mixture of 80 wt.% oxide, 10 wt.% carbon black (N660, Repsol) and 10 wt.% PTFE. Lithium electrodes consisted of a metallic lithium disc. The electrolyte solution (1 M $LiClO_4$ in bidistilled PC) was supported on porous glass-paper discs. The galvanostatic cycling experiments of lithium anode and rocking chair cells were carried out at $C/60$ and $C/40$ rates, respectively.

### 2.3. X-ray diffraction and Mössbauer spectroscopy

The purity and the structure of pristine and modified phases and their corresponding lithiated products were checked by X-ray powder diffractometry (XPD) using a Siemens D500 diffractometer furnished with Cu Kα radiation and graphite monochromator.

Mössbauer spectra of polycrystalline samples were measured using an EG&G WISSEL MA260 constant acceleration spectrometer. The γ-ray source was $^{119m}Sn$ in a $BaSnO_3$ matrix, used at room temperature. Cooled samples at 80 K were studied by using a liquid nitrogen cryostat. The scale velocity was calibrated by using a $^{57}Co$ source and a metallic iron foil as absorber. The spectra were fitted to Lorentzian profiles by a least-squares method. The goodness of fit was controlled by $\chi$-squared and misfit tests [17]. All isomer shifts reported here are given with respect to the centre of a $BaSnO_3$ standard absorber.

## 3. Results and discussion

The spinel compounds with $Cu_2CoSn_3S_8$ and $CuCoSn_3S_8$ stoichiometries were characterized by chemical analysis and profile fitting of XPD data by the Rietveld method, as described in Ref. [15]. Their cation distribution in the $Fd\bar{3}m$ space group can be summarized as: $(Cu_8)_{8a}[Co_4Sn_{12}]_{16d}S_{32}$ and $(Cu_4\square_4)_{8a}[Co_4Sn_{12}]_{16d}S_{32}$, respectively. The $^{119}Sn$ Mössbauer spectra for $Cu_2CoSn_3S_8$ showed a quadrupole doublet characteristic of $Sn^{IV}$ (Table 1). A very slight decrease in the isomer shift ($\delta = 1.194(2)$ mm $s^{-1}$) was observed for $CuCoSn_3S_8$ after copper extraction; this can be interpreted as due to a small decrease in the covalent character of the Sn–S bonding. From these results, it can be derived the existence of only $Co^{2+}$ in $Cu_2CoSn_3S_8$ and only $Co^{3+}$ in $CuCoSn_3S_8$. These ions together with $Sn^{4+}$ ions are randomly distributed in 16d octahedral sites. Copper is then in the form of $Cu^+$ ions which occupy the 8a tetrahedral sites defined by the anion array. Thus, 16c octahedral, 8b and 48f tetrahedral interstices are empty, providing a suitable path for lithium diffusion and accomodation. Moreover, cation vacancies in the tetrahedral 8a sites of $CuCoSn_3S_8$ may decrease the repulsions exerted by copper ions on the incoming lithium ions.

$CuCoSn_3S_8$ and $Cu_2CoSn_3S_8$ were evaluated as the active electrode material in lithium anode cells. Two-electrode lithium cells were studied by step potential electrochemical spectroscopy. The voltage–composition and cell current–composition plots for the two cells are shown in Fig. 1. For the $CuCoSn_3S_8$ spinel, cell current–composition curves

Table 1
$^{119}Sn$ Mössbauer parameters of $Li_xCu_2CoSn_3S_8$ and $Li_xCuCoSn_3S_8$ ($x = 0, 4$) spinel compounds [a]

| | | $Li_xCu_2CoSn_3S_8$ | $Li_xCuCoSn_3S_8$ |
|---|---|---|---|
| $x=0$, $Sn^{IV}$ | $\delta$ | 1.202(1) | 1.194(2) |
| | $\Delta$ | 0.318(6) | 0.34(1) |
| | $\Gamma$ | 0.863(6) | 0.95(1) |
| | $C$ | 100 | 100 |
| $x=2$, $Sn^{IV}$ | $\delta$ | 1.220(3) | 1.192(3) |
| | $\Delta$ | 0.35(1) | 0.33(2) |
| | $\Gamma$ | 0.95(1) | 0.94(2) |
| | $C$ | 94(1) | 100 |
| $x=2$, $Sn^{II}$, ~6% | $\delta$ | 3.1(1) | |
| | $\Delta$ | 1.0(1) | |
| | $\Gamma$ | 1.9(4) | |
| | $C$ | 6(1) | |
| $x=4$, $Sn^{IV}$ | $\delta$ | 1.205(4) | 1.191(3) |
| | $\Delta$ | 0.36(2) | 0.32(2) |
| | $\Gamma$ | 0.90(1) | 0.97(2) |
| | $C$ | 86(1) | 95(1) |
| $x=4$, $Sn^{II}$, ~6% | $\delta$ | 3.16(5) | 3.28(9) |
| | $\Delta$ | 0.6(2) | 0.6(3) |
| | $\Gamma$ | 1.3(2) | 1.1(4) |
| | $C$ | 14(1) | 5(1) |

[a] $\delta$ = isomer shift relative to $BaSnO_3$, $\Delta$ = quadrupole splitting, $\Gamma$ = full width at half maximum, $C$ = contribution in %. All parameters are expressed in mm $s^{-1}$.

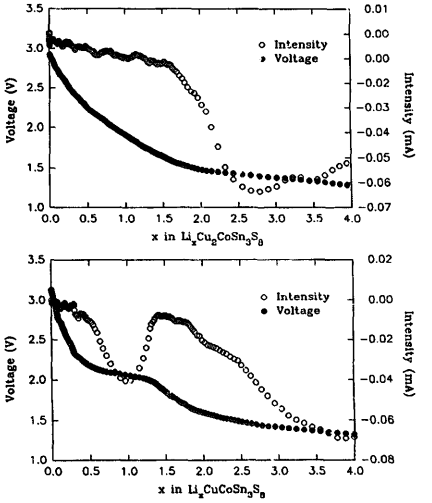


Fig. 1. Results of the step potential electrochemical spectroscopy of lithium anode cells using two different thiospinel compositions as cathode material.

revealed a first $Co^{III}/Co^{II}$ reduction peak during cell discharge at about 1.0 F $mol^{-1}$, which is consistent with the pseudo-plateau observed in the V–$x$ curve. On the contrary, the more steep decrease in voltage between $x=0$ and $x=2$, which is observed for the $Cu_2CoSnS_8$ composition, reveals a lower potential reduction process as compared with the $CuCoSn_3S_8$ composition. The XPD patterns of lithium intercalated $Cu_2CoSn_3S_8$ showed the occurrence of copper metal reflections which are indicative of a copper extraction process simultaneous to lithium insertion during the first steps of discharge. This behaviour can be considered as a consequence of the lower oxidation state of cobalt in the copper-rich spinels, the repulsions exerted on tetrathedrally coordinated ions by the inserting lithium ions and the large difussivity and ease of the reduction of copper ions.

For both sulfide compositions, the extended pseudo-plateau observed during the discharge of the cells above 2 F $mol^{-1}$ (Fig. 1) is consistent with $^{119}Sn$ Mössbauer spectroscopy data which showed the gradual occurrence of a new signal in the range of 3.00 mm $s^{-1}$ attributable to $Sn^{II}$ [15] (Table 1). According to these results, the reduction of tin atoms takes place during prolongued insertion after $Cu^{I}/Cu^{0}$ reduction– extraction from $Cu_2CoSn_3S_8$ and after $Co^{III}/Co^{II}$ reduction in $CuCoSn_3S_8$ compositions. Nevertheless, this process was accompanied by a progressive loss of long-range order, as reflected by decreasing signal to background ratios in the XPD patterns which may have undesired effects on insertion reversibility and cell cycleability.

On the other hand, current relaxation was followed during each step of the potentiostatic experiment (see Fig. 2). In these plots it can be observed that current decreases more abruptly for the $Cu_2CoSn_3S_8$ composition.

The lithium-ion diffusion coefficients were obtained from the potentiostatic measurements, according to the method described in Ref. [18]. From the logarithm plots of cell current–time, the slopes obtained for long relaxation times were used to obtain the diffusion coefficient $D$, according to the expression

$$\mathrm{d}\log|i|/\mathrm{d}t = -1.071\, D/L^{2} \qquad (1)$$

The $D$ values computed by this procedure are plotted versus the lithium content in Fig. 3. From this plot it is noteworthy that the changes with composition $x$ do not follow a clear trend for each spinel sulfide. This is an expected result if the large number of empty sites which are available for lithium ions in the structure is compared with the limited depth of discharge studied here. This avoids the effects enhanced $Li^{+}$–$Li^{+}$ repulsions which commonly decrease the $D$ values for extended insertion [19]. On the other hand, larger coefficients are found for the copper extracted thiospinel in the $0<x<2$ interval as compared with the copper-rich composition. This is consistent with the effect of cation vacancies in 8a sites in $CuCoSn_3S_8$, as reported in other copper-extracted spinel compounds [13,14].

Having in mind the above results, the galvanostatic experiments were carried out on lithium and lithium-ion cells by using the chemically copper-extracted product as the electrode material. The galvanostatic cycling behaviour in the 2–

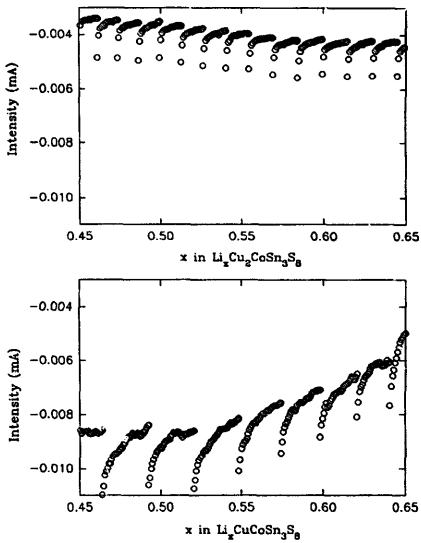


Fig. 2. Current relaxation in potential steps corresponding to similar values of lithium content for the two sulfide compositions.

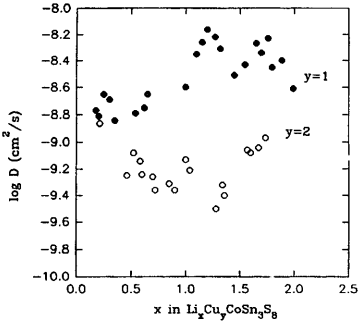


Fig. 3. Plot of the lithium-ion diffusion coefficients vs. lithium content.

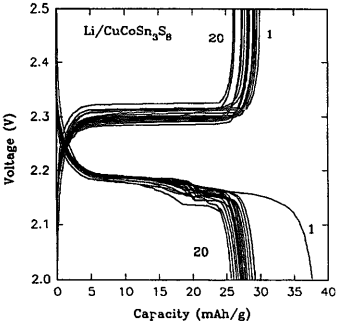


Fig. 4. Galvanostatic cycling of lithium anode cells using $CuCoSn_3S_8$ electrodes in the 2.0–2.5 V potential window.

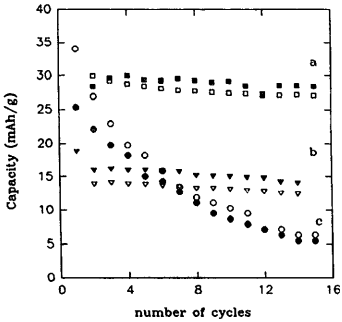


Fig. 5. Plot of cell capacity vs. cycle number: (a) $Li/LiClO_4(PC)/CuCoSn_3S_8$ cell in the 2–2.5 V potential window; (b) $LiCoO_2/LiClO_4(PC)/CuCoSn_3S_8$ cell in the 1.0–2.0 V potential window of the sulfide electrode as referred to a lithium metal electrode, and (c) $Li/LiClO_4(PC)/CuCoSn_3S_8$ cell in the 1.8–3.4 V potential window.

2.5 V potential window is shown in Fig. 4 for a lithium anode cell. Cell capacity, as referred to the mass of active material, takes values of about 30 mAh $g^{-1}$, as referred to the complete mass of the active eletrode materials. This value is about 83% of the theoretical capacity, which can be calculated from the equation

$$CuCoSn_3S_8 + Li = LiCuCoSn_3S_8 \quad (2)$$

In addition to the initial capacity loss from the first to the second cycle of about 9 mAh $g^{-1}$, the following ten cycles lead to little capacity losses. This was also found for further cycling, as shown in the plot of capacity–number of cycles which is included in Fig. 5(a). Moreover, the appropriate selection of the potential window is crucial for the good cycling properties of this material, as evidenced in Fig. 5(c). By selecting a 1.8–3.4 V range in the cycling experiments, a dramatic decrease in capacity is observed. It should be noted that although lithium is inserted throughout all this interval, as shown by Fig. 1, the irreversible process of loss of a long-range ordering found for $x$ values larger than 3 restricts the cycling properties.

On the other hand, the intermediate cell voltages observed in lithium cells make $CuCoSn_3S_8$ a promising candidate for either lithium anode cells or rocking chair cells, provided that the positive intercalation electrode is chosen with sufficiently high potential range of intercalation. That is the case of $LiCoO_2$, a material which can be considered as standard electrode in lithium-ion cells. Although cell voltages were slightly lower for the copper-rich compound (Fig. 1), the lower diffusivity and the irreversible copper extraction during lithium insertion allowed us to discard this composition for use in lithium-ion cells.

Three electrode sulfide/$LiClO_4$(PC)/$LiCoO_2$ rocking chair cells using lithium auxiliary electrode were examined by galvanostatic cycling experiments. Two factors were taken into account in order to optimize the rocking chair cell: (i) the voltage limits for efficient cycling (see Fig. 5), and (ii) the relative amount of positive and negative electrode material. This can be represented by the $r = m^+/m^-$ ratio, where $m^+$ and $m^-$ are the weight of cathode and anode active materials, respectively. This ratio has to be adjusted in such a way that the reversible capacity of each electrode is equalized for both the safety and the optimum performance. In other words, when the cathode is fully charged (delithiated), the negative intercalation electrode has to be fully lithiated with its voltage close to its lower limit versus lithium.

The initial choice of $r$ value and voltage limits were made according to theoretical consideration taking into account the electrochemical behaviour of each compounds versus lithium anode tested in previous research. Nevertheless, the polarization of the lithium electrode which takes place in a lithium anode cell is not present in a rocking chair battery. Consequently, the optimum $r$ value should be found empirically.

The optimum ratio was found to take a value of $r = 0.9$. For this ratio, cell voltages were close to 1.3 V during cell discharge and to 1.8 V during cell charge (Fig. 6). Cell

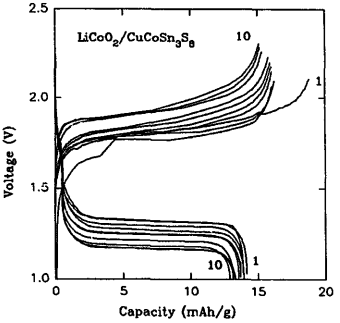


Fig. 6. Galvanostatic cycling of the rocking chair $LiCoO_2/LiClO_4(PC)/CuCoSn_3S_8$ cell in the 1.0–2.0 V potential window of the sulfide electrode as referred to a lithium metal electrode.

capacity, as referred to the weight of the complete cell, is about 13 mAh $g^{-1}$. This value is about 50% of the theoretical capacity, which can be calculated from the equation

$$LiCuCoSn_3S_8 + 2Li_{0.5}CoO_2 = CuCoSn_3S_8 + 2LiCoO_2 \quad (3)$$

The theoretical and observed capacities of the lithium and lithium-ion cells studied here are below the values found for different commercial rechargeable batteries, such as the coke/$LiCoO_2$ commercial rocking chair system (theoretical cell capacity 95 mAh $g^{-1}$). Also, the spinel chalcogenides studied here, as the most active electrode materials, are more expensive than coke electrodes. Nevertheless, the good cycling properties make this material a potential candidate for those applications in which cell weight is not a limiting factor.

Finally, an additional positive factor in the use of these spinel materials as insertion electrodes comes from the presence of $Sn^{IV}$ ions, which are suitable for reduction at potentials slightly lower than the working voltage. This feature may be of interest as an overdischarge protection of the cells.

## Acknowledgements

The authors acknowledge the financial support of EC (Contract JOU2-CT93-0326), CICYT (MAT94-1155-CE) and Foreign Office (France) for the Picasso program.

## References

[1] B. Di Pietro, M. Patriarca and B. Scrosati, *J. Power Sources, 8* (1982) 298.
[2] J.J. Auborn and Y.L. Barbario, *J. Electrochem. Soc., 134* (1987) 638.
[3] K.M. Abraham, D.M. Pasquariello and E.B. Willstaedt, *J. Electrochem. Soc., 137* (1990) 743.
[4] T. Nagaura and K. Tazawa, *Prog. Batteries Solar Cells, 9* (1990) 20.
[5] J.R. Dahn, U. von Sacken, H. Al Janaby and M.K. Juzkow, *J. Electrochem. Soc., 138* (1991) 2207.
[6] D. Guyomard and J.M. Tarascon, *J. Electrochem. Soc., 139* (1992) 937.
[7] T. Ohzuku, Y. Iwakoshi and K. Sawai, *J. Electrochem. Soc., 140* (1993) 2490.
[8] E. Ferg, R.J. Gummow, A. de Kock and M.M. Thackeray, *J. Electrochem. Soc., 141* (1994) L147.
[9] E.D. Plichta and W.K. Behl, *J. Electrochem Soc., 140* (1993) 46.
[10] M. Eisenberg, *J. Electrochem. Soc., 127* (1980) 2382.
[11] M. Inaba, Z. Siroma, Z. Ogumi, T. Abe, Y. Mizutani and M. Asano, *Chem. Lett.*, (1995) 661.
[12] R. Schöllhorn and A. Payer, *Angew. Chem. Int. Ed., 24* (1985) 67.
[13] A.C.W.P. James, B. Ellis and J.B. Goodenough, *Solid State Ionics, 18/19* (1986) 1068.
[14] N. Imanishi, K. Inoue, Y. Takeda and O. Yamamoto, *J. Power Sources 43–44* (1993) 619.
[15] P. Lavela, J.L. Tirado, J. Morales, J. Olivier Fourcade and J.C. Jumas, *J. Mater. Chem. 6* (1996) 41.
[16] W.D. Johnston, R.R. Heikes and S. Sestrich, *J. Phys. Chem. Solids, 7* (1959) 1
[17] K. Rubenbauer and T. Birchall, *Hyperf. Inter., 7 (1979) 125.*
[18] C.J. Wen, B.A. Boukamp, R.A. Huggins and W. Weppner, *J. Electrochem. Soc., 126* (1979) 2258.
[19] A.S. Nagelberg, *Ph.D. Thesis*, University of Pennsylvania, Philadelphia, PA, USA, 1978.